

CLImage: Human-Annotated Datasets for Complementary-Label Learning

Hsiu-Hsuan Wang, Tan-Ha Mai, Nai-Xuan Ye, Wei-I Lin, Hsuan-Tien Lin
National Taiwan University
{b09902033, d10922024, b09902008, r10922076, htlin}@csie.ntu.edu.tw

Abstract

Complementary-label learning (CLL) is a weakly-supervised learning paradigm that aims to train a multi-class classifier using only complementary labels, which indicate classes to which an instance does not belong. Despite numerous algorithmic proposals for CLL, their practical applicability remains unverified for two reasons. Firstly, these algorithms often rely on assumptions about the generation of complementary labels, and it is not clear how far the assumptions are from reality. Secondly, their evaluation has been limited to synthetic datasets. To gain insights into the real-world performance of CLL algorithms, we developed a protocol to collect complementary labels from human annotators. Our efforts resulted in the creation of four datasets: CLCIFAR10, CLCIFAR20, CLMicroImageNet10, and CLMicroImageNet20, derived from well-known classification datasets CIFAR10, CIFAR100, and TinyImageNet200. These datasets represent the very first real-world CLL datasets. Through extensive benchmark experiments, we discovered a notable decrease in performance when transitioning from synthetic datasets to real-world datasets. We investigated the key factors contributing to the decrease with a thorough dataset-level ablation study. Our analyses highlight annotation noise as the most influential factor in the real-world datasets. In addition, we discover that the biased-nature of human-annotated complementary labels and the difficulty to validate with only complementary labels are two outstanding barriers to practical CLL. These findings suggest that the community focus more research efforts on developing CLL algorithms and validation schemes that are robust to noisy and biased complementary-label distributions.

1 Introduction

Ordinary multi-class classification methods rely heavily on high-quality labels to train effective classifiers. However, such labels can be expensive and time-consuming to collect in many real-world applications. To address this challenge, researchers have turned their attention towards weakly-supervised learning, which aims to learn from incomplete, inexact, or inaccurate data sources [21, 29]. This learning paradigm includes but is not limited to noisy-label learning [6],

partial-label learning [2], positive-unlabeled learning [4], and complementary-label learning [9].

In this work, we focus on complementary-label learning (CLL). This learning problem involves training a multi-class classifier using only complementary labels, which indicate the classes that a data instance does not belong to. Although several algorithms have been proposed to learn from complementary labels, they were only benchmarked on synthetic datasets with some idealistic assumptions on complementary-label generation [1, 9, 10, 17, 22]. Thus, it remains unclear how well these algorithms perform in practical scenarios.

In particular, current CLL algorithms heavily rely on the *uniform assumption* for generating complementary labels [9], which specifies that complementary labels are generated by uniformly sampling from the set of all possible complementary labels. To alleviate the restrictiveness of the uniform assumption, Yu et al. [28] considered a more general *class-conditional assumption*, where the distribution of the complementary labels only depends on its ordinary labels. These assumptions have been used in many subsequent works to generate the *synthetic complementary datasets* for examining CLL algorithms [1, 10, 17, 22, 26]. Although these assumptions simplify the design and analysis of CLL algorithms, it remains unknown whether these assumptions hold true in practice and whether violation of these assumptions will significantly affect the performance of CLL algorithms. In addition to the uniform or class-conditional assumptions, most existing studies implicitly assumes that the complementary labels are noise-free. That is, they do not mistakenly represent the ordinary labels. While some studies claim to be more robust to noisy complementary labels [15], they were only tested on synthetic scenarios. It remains unclear how noisy the real-world datasets are, and how such noise affects the performance of current CLL algorithms.

To understand how much the real-world scenario differs from the assumptions, we started by collecting the datasets CLCIFAR10 and CLCIFAR20, which are derived from the famous CIFAR datasets for ordinary multi-class classification [13]. Since their release in 2023, the datasets [23] have been utilized by several emerging CLL studies [16, 24, 25, 27], demonstrating their instantaneous impact. We continue to extend the collection and form two additional human-annotated datasets, CLMicroImageNet10 and CLMicroImageNet20, which are derived from TinyImageNet200 [14, 20]. The extension verifies that our observations on CIFAR-derived datasets hold true for other image datasets. For all four datasets, we analyze the collected complementary labels, including their noise rates and non-uniform nature. Then, we perform benchmark experiments with diverse state-of-the-art CLL algorithms and conduct dataset-level ablation study on the assumptions of complementary-label generation using the collected datasets. Our studies reveal annotation noise as the most influential factor in the real-world datasets, and confirm that the non-uniform nature of human-annotated complementary labels cause certain CLL algorithms more susceptible to overfitting. These findings immediately suggest that the community focus more research efforts on developing CLL algorithms that are robust to noisy and non-uniform complementary-label distributions. In addition, we used the collected datasets to demonstrate that existing complementary-label-only validation schemes are

not mature yet, suggesting the community a novel research direction for making CLL practical. Our contributions are summarized as follows:

- We designed a collection protocol of complementary labels (CLs) for images, and verified that the protocol collects reasonable human-annotated CLs across different datasets.
- We released **CLImage**, the collected set of four real-world CL datasets to support the continuous research of the community, publicly released at https://github.com/ntucllab/CLImage_Dataset.
- We analyzed the collected datasets with extensive benchmarking experiments, which provides novel and valuable insights for the community.

2 Preliminaries on CLL

2.1 Complementary-label learning

In ordinary multi-class classification, a dataset $D = \{(\mathbf{x}_i, y_i)\}_{i=1}^n$ that is *i.i.d.* sampled from an unknown distribution is given to the learning algorithm. For each i , $\mathbf{x}_i \in \mathbb{R}^M$ represents the M -dimension feature of the i -th instance and $y_i \in [K] = \{1, 2, \dots, K\}$ represents the class \mathbf{x}_i belongs to. The goal of the learning algorithm is to learn a classifier from D that can predict the labels of unseen instances correctly. The classifier is typically parameterized by a scoring function $\mathbf{g}: \mathbb{R}^M \rightarrow \mathbb{R}^K$, and the prediction is made by $\arg \max_{k \in [K]} \mathbf{g}(\mathbf{x})_k$ given an instance \mathbf{x} , where $\mathbf{g}(\mathbf{x})_k$ denotes the k -th output of $\mathbf{g}(\mathbf{x})$. In contrast to ordinary multi-class classification, CLL shares the same goal of learning a classifier but trains with different labels. In CLL, the ordinary label y_i is not accessible to the learning algorithm. Instead, a complementary label \bar{y}_i is provided, which is a class that the instance \mathbf{x}_i does *not* belong to. The goal of CLL is to learn a classifier that is able to predict the correct labels of unseen instances from a complementary-label dataset $\bar{D} = \{(\mathbf{x}_i, \bar{y}_i)\}_{i=1}^n$.

2.2 Common assumptions on CLL

Researchers have made some additional assumptions on the generation process of complementary labels to facilitate the analysis and design of CLL algorithms. One common assumption is the *class-conditional assumption* [28]. It assumes that the distribution of a complementary label only depends on its ordinary label and is independent of the underlying example’s feature, i.e., $P(\bar{y}_i | \mathbf{x}_i, y_i) = P(\bar{y}_i | y_i)$ for each i . One special case of the class-conditional assumption is the *uniform assumption*, which further specifies that the complementary labels are generated uniformly. That is, $P(\bar{y}_i = k | y_i = j) = \frac{1}{K-1}$ for all $k \in [K] \setminus \{j\}$ [9, 10, 15].

For convenience, a $K \times K$ matrix T , called *transition matrix*, is often used to represent how the complementary labels are generated under the class-conditional assumption. $T_{j,k}$ is defined to be the probability of obtaining a complementary label k if the underlying ordinary label is j , i.e., $T_{j,k} = P(\bar{y} = k | y = j)$ for

each $j, k \in [K]$. The diagonals of T hold the conditional probabilities that a complementary label mistakenly represents the ordinary label. That is, they indicate the noise level of the complementary labels. When T contains all zeros on its diagonals, the CLL scenario is called *noiseless*. For instance, the uniform and noiseless assumption can be represented by $T_{j,j} = 0$ for each $j \in [K]$ and $T_{j,k} = \frac{1}{K-1}$ for each $k \neq j$. Class-conditional CLL scenarios based on any other non-uniform T are often called *biased*.

2.3 A brief overview of CLL algorithms

The pioneering work by Ishida et al. [9] studied how to learn from complementary labels under the *uniform assumption* by converting the risk estimator in ordinary multi-class classification to an unbiased risk estimator (**URE**) in CLL [9]. **URE** is then found to be prone to overfitting because of negative empirical risks, and is upgraded with two tricks, non-negative risk estimator (**URE-NN**) and gradient ascent (**URE-GA**) [10]. The *surrogate complementary loss* (**SCL**) algorithm mitigates the overfitting issue of **URE** by a different loss design that decreases the variance of the empirical estimation. However, these algorithms either rely on the uniform assumption in design or are only tested on the synthetic datasets that obeys the uniform assumption.

To make CLL one step closer to practice, researchers have explored algorithms to go beyond the uniform (and thus noiseless) assumption. Yu et al. [28] utilized the forward-correction loss (**FWD**) to accommodate biased complementary label generation by adapting techniques from noisy label learning [19] to change the loss. Additionally, Gao and Zhang [7] proposed the **L-W** algorithm based on discriminatively modeling the distribution of complementary labels through a weighting function, further improving the performance in bias scenario. Furthermore, Ishiguro et al. [11] designed robust loss functions for learning from noisy CLs, including **MAE** and **WMAE**, by applying the gradient ascent technique [10] to handle noisy scenarios.

Besides CLL algorithms, a crucial component for making CLL practical is model validation. In ordinary-label learning, this can be done by naively calculating the classification accuracy on a validation dataset. In CLL, this scheme can be intractable if there are not enough ordinary labels. One generic way of model validation is based on the result of Ishida et al. [10] by calculating the unbiased risk estimator of the zero-one loss, i.e.,

$$\hat{R}_{01}(\mathbf{g}) = \frac{1}{N} \sum_{i=1}^N e_{\bar{y}_i}^\top (T^{-1}) \ell_{01}(\mathbf{g}(x_i)) \quad (1)$$

where $e_{\bar{y}_i}$ denotes the one-hot vector of \bar{y}_i , $\ell_{01}(\mathbf{g}(x_i))$ denotes the K -dimensional vector $(\ell_{01}(\mathbf{g}(x_i), 1), \dots, \ell_{01}(\mathbf{g}(x_i), K))^T$, and $\ell_{01}(\mathbf{g}(x_i), k) = 0$ if $\arg \max_{k \in [K]} \mathbf{g}(x_i) = k$ and 1 otherwise, representing the zero-one loss of $\mathbf{g}(x_i)$ if the ordinary label is k . This estimator will be used in the experiments in Section 6. Another validation objective, surrogate complementary estimation loss (SCEL), was proposed by Lin and Lin [15]. SCEL measures the log loss of the complementary probability

estimates induced by the probability estimates on the ordinary label space. The formula to calculate SCEL is as follows,

$$\hat{R}_{\text{SCEL}}(\mathbf{g}) = \frac{1}{N} \sum_{i=1}^N -\log \left(e_{y_i}^\top T^\top \text{softmax}(\mathbf{g}(x_i)) \right). \quad (2)$$

3 Construction of the CLImage collection

In this section, we introduce the four complementary-labeled datasets that we collected, CLCIFAR10, CLCIFAR20, CLMicroImageNet10 and CLMicroImageNet20. All datasets are labeled by human annotators on Amazon Mechanical Turk (MTurk)¹.

3.1 Datasets and goals

The complementary-labeled datasets are derived from ordinary multi-class classification datasets. CIFAR10, CIFAR100 and TinyImageNet200 [13, 14, 20]. This selection is motivated by the real-world noisy label dataset by Wei et al. [26]. Building upon the CIFAR and TinyImageNet200 datasets allow us to estimate the noise rate and the empirical transition matrix easily, as they already contain nearly noise-free ordinary labels. In addition, many of the state-of-the-art CLL algorithms have been benchmarked on synthetic complementary labels with the CIFAR datasets [5, 12, 18]. Our CLCIFAR counterparts immediately allow a fair comparison to those results with the same network architecture.

In addition to our CLCIFAR extensions, we are the first to introduce (Tiny)ImageNet-derived datasets to the CLL literature. Such datasets serve two purposes. First, it allows us to confirm the validity of our collection protocol and findings beyond CIFAR-derived datasets. Second, ImageNet knowingly contains images of higher complexity than CIFAR and can thus be used to challenge the ability of existing CLL algorithms more realistically.

There is a historical note that is worth sharing with the community: We initially attempted to collect complementary labels based on the 100 classes in CIFAR100. But some preliminary testing soon revealed that state-of-the-art CLL algorithms cannot produce meaningful classifiers for 100 classes even on synthetic complementary labels that are uniformly and noiselessly generated. We thus set our collection goals to be 10-class classification, which is the focus of most current CLL studies, and 20-class classification, which extends the horizon of CLL and matches the 20 super-class structure in CIFAR.

3.2 Complementary label collection protocol

To collect only complementary labels from the CIFAR, TinyImageNet datasets, for each image in the training split, we first randomly sample four distinct labels and ask the human annotators to select any of the *incorrect* one from them. To

¹<https://www.mturk.com/>

leave room for analyzing the annotators’ behavior, each image is labeled by three different annotators. The four labels are re-sampled for each annotator on each image. That is, each annotator possibly receives a different set of four labels to choose from. An algorithmic description of the protocol is as follows. For each image \mathbf{x} ,

1. Uniformly sample four labels without replacement from the label set $[K]$.
2. Ask the annotator to select any one of the complementary label \bar{y} from the four sampled labels.
3. Add the pair (\mathbf{x}, \bar{y}) to the complementary dataset.

Note that if the annotators always select one of the correct complementary labels uniformly, the empirical transition matrix will also be uniform in expectation. We will inspect the empirical transition matrix in Section 4. The labeling tasks are deployed on MTurk by dividing them into smaller we first divide the total images into smaller human intelligence tasks (HITs). For instance, for constructing the CLCIFAR datasets, we first divide the 50,000 images into five batches of 10,000 images. Then, each batch is further divided into 1,000 HITs with each HIT containing 10 images. Each HIT is deployed to three annotators, who receive 0.03 dollar as the reward by annotating 10 images. To make the labeling task easier and increase clarity, the size of the images are enlarged to 200×200 pixels.

4 Result analysis

Next, we closely examine the collected complementary labels. We first analyze the error rates of the collected labels, and then verify whether the transition matrix is uniform or not. Finally, we end with an analysis on the behavior of the human annotators observed in the label collection protocol.

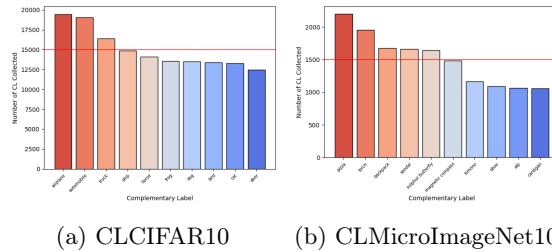


Figure 1: The label distribution of CLCIFAR10 and CLMicroImageNet10 datasets.

Observation 1: noise rate compared to ordinary label collection We first look at the noise rate of the collected complementary labels. A complementary label is considered to be incorrect if it is actually the ordinary label. The mean error rate made by the human annotators is 3.93% for CLCIFAR10, 2.80%

for CLCIFAR20, 5.19% for CLMicroImageNet10 and 3.21% for CLMicroImageNet20. In theory, we can estimate a random annotator achieves a noise rate of $\frac{1}{K}$ for complementary label annotation and a noise rate of $\frac{K-1}{K}$ for ordinary label annotation. If we compare the human annotators to a random annotator, then for CLCIFAR10, human annotators have 60.7% less noisy labels than the random annotator whereas for CIFAR10-N, human annotators have 80% less noisy labels. This demonstrates that human annotators are more competent compared to a random annotator in the ordinary-label annotation. Similarly, human annotators have 44% less noise than a random annotator for CLCIFAR20 and 73.05% less noise for CIFAR100N-coarse. This observation reveals that while the absolute noise rate is lower in annotating complementary labels, it may be more difficult to be competent against random labels than the ordinary label annotation.

Observation 2: imbalanced complementary label annotation Next, we analyze the distribution of the collected complementary labels. The frequency of the complementary labels for the CLCIFAR10 and CLMicroImageNet10 (CLMIN10) datasets are reported in Figure 1. As we can see in the figure, the annotators exhibit specific biases towards certain labels. For instance, in CLCIFAR10, annotators prefer "airplane" and "automobile," while in CLMIN10, they prefer "pizza" and "torch". In CLCIFAR10, the bias is towards labels in different categories, as vehicles ("airplane," "automobile") versus animals ("cat", "bird"). In contrast, in CLMIN10, the bias is towards items that are easily recognizable ("pizza" and "torch") and against those that are less familiar ("cardigan" or "alp").

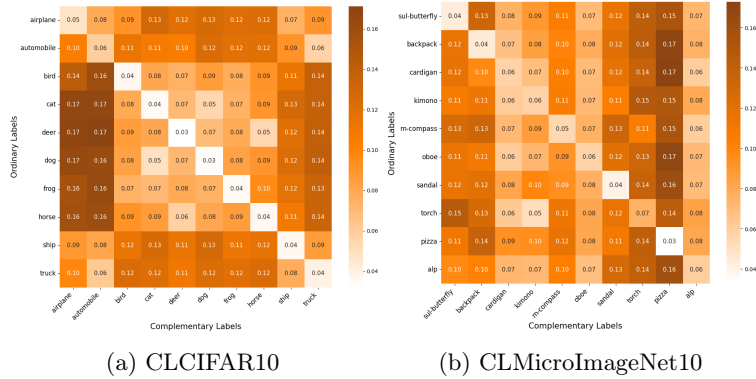


Figure 2: The empirical transition matrices of CLCIFAR10 and CLMicroImageNet10.

Observation 3: biased transition matrix Finally, we visualize the empirical transition matrix using the collected CLs in Figure 2. Based on the first two observations, we could imagine that the transition matrix is biased. By inspecting Figure 2, we further discover that the bias in the complementary labels are dependent on the true labels. For instance, in CLCIFAR10, despite we

see more annotations on airplane and automobile in aggregate, conditioning on the transportation-related labels (“airplane”, “automobile”, etc), the distribution of the complementary labels becomes more biased towards other animal-related labels (“bird”, “cat”, etc.) Furthermore, this observation holds true on CLMIN10 as well. Next, we study the impact of the bias and noise on existing CLL algorithms.

We discovered similar patterns in all four human-annotated datasets, validating that our design methodology is practical for collecting real-world CLL image datasets. Due to space limitations, we have included the detailed analysis of CLCIFAR20 and CLMicroImageNet20 in Appendix B.4.

5 Experiments

In this section, we benchmarked several state-of-the-art CLL algorithms on CLImage. A significant performance gap between the models trained on the humanly annotated CLCIFAR, CLMicroImageNet dataset and those trained on the synthetically generated complementary labels (CL) was observed in Section 5.1, which motivates us to analyze the possible reasons for the gap with the following experiments. To do so, we discuss the effect of three factors in the label generating process, feature dependency, noise, and biasedness, in Section 5.2, Section 5.3, and Section 5.4, respectively. From our experiment results, we conclude that noise is the dominant factor affecting the performance of the CLL algorithms on CLCIFAR².

5.1 Standard benchmark on CLImage

Baseline methods Several state-of-the-art CLL algorithms were selected for this benchmark. Some of them take the transition matrix T as inputs, which we call **T -informed** methods, including two version of forward correction [28]: **FWD-U** and **FWD-R**, two version of unbiased risk estimator with gradient ascent [10]: **URE-GA-U** and **URE-GA-R**, and robust loss [11] for learning from noisy CL: **CCE**, **MAE**, **WMAE**, **GCE**, and **SL**³. We also included some algorithms that assume the transition matrix T to be uniform, called **T -agnostic** methods, including surrogate complementary loss **SCL-NL** and **SCL-EXP** [1], discriminative modeling **L-W** and its weighted variant (**L-UW**) [7], and pairwise-comparison (**PC**) with the sigmoid loss [9]. The details of the algorithms mentioned above are discussed in Appendix D.

Implementation details We collected and released three CLs per image to prepare for future studies. However, for this standard benchmark, we chose the first CL from the collected labels for each data instances to form a single CLL dataset, ensuring reproducibility. Then, we trained a ResNet18 [8] model

²Due to space and time constraints, we only provide the results and discussion on the CLCIFAR datasets.

³Due to space limitations, we only provided the results of MAE. The remaining results and discussions related to the robust loss methods can be found in Appendix B.3

Table 1: Standard benchmark results on CLCIFAR/ CLMicroImageNet(CLMIN) and uniform-CIFAR/ MicroImageNet(MIN) datasets. Mean accuracy (\pm standard deviation) on the testing dataset from four trials with different random seeds. Highest accuracy in each column is highlighted in bold.

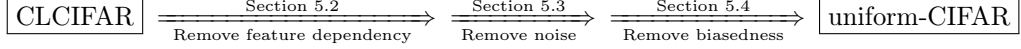
	uniform-CIFAR10	uniform-CIFAR20	uniform-MIN10	uniform-MIN20	CLCIFAR10	CLCIFAR20	CLMIN10	CLMIN20
FWD-U	64.19\pm0.57	21.54 \pm 0.37	36.30 \pm 1.12	12.57 \pm 2.94	34.83 \pm 0.50	8.03 \pm 0.74	23.85 \pm 2.76	6.33 \pm 1.04
FWD-R	61.32 \pm 0.90	21.50 \pm 0.38	35.70 \pm 1.19	14.85\pm1.75	38.13\pm0.88	20.27\pm0.53	30.15\pm1.83	10.60\pm0.82
URE-GA-U	50.24 \pm 1.11	16.67 \pm 1.35	35.70 \pm 1.97	11.65 \pm 1.90	34.72 \pm 0.40	10.49 \pm 0.52	22.90 \pm 2.97	5.75 \pm 0.43
URE-GA-R	50.73 \pm 1.83	17.57 \pm 0.61	33.65 \pm 1.40	9.78 \pm 3.88	30.23 \pm 0.70	6.17 \pm 0.82	13.25 \pm 5.11	6.50 \pm 0.35
SCL-NL	63.76 \pm 0.09	21.37 \pm 1.18	37.05\pm1.40	13.00 \pm 2.80	34.77 \pm 0.60	8.02 \pm 0.36	21.80 \pm 1.85	6.17 \pm 0.49
SCL-EXP	63.29 \pm 1.02	21.57\pm1.13	36.55 \pm 1.28	12.95 \pm 3.38	35.18 \pm 0.67	7.70 \pm 0.41	24.80 \pm 1.14	5.58 \pm 0.13
L-W	54.32 \pm 0.41	19.59 \pm 0.99	33.80 \pm 2.66	12.70 \pm 2.35	32.99 \pm 1.01	7.71 \pm 0.35	23.80 \pm 2.64	6.40 \pm 0.29
L-UW	57.52 \pm 0.59	20.71 \pm 0.92	35.10 \pm 2.74	12.12 \pm 3.13	34.69 \pm 0.32	8.15 \pm 0.30	22.40 \pm 1.67	6.35 \pm 0.86
PC-sigmoid	37.78 \pm 0.80	14.48 \pm 0.47	29.10 \pm 0.98	10.72 \pm 1.38	32.15 \pm 0.80	12.11 \pm 0.46	23.15 \pm 0.46	6.90 \pm 1.04
ROB-MAE	59.38 \pm 0.63	18.17 \pm 1.31	31.50 \pm 1.81	6.35 \pm 0.86	20.23 \pm 1.02	5.40 \pm 0.59	14.15 \pm 0.68	5.38 \pm 0.33
	CIFAR10		CIFAR20		MIN10		MIN20	
standard supervision	82.80 \pm 0.28		63.80 \pm 0.49		68.70 \pm 1.53		63.90 \pm 1.00	

using the baseline methods mentioned above on the single CLL dataset using the Adam optimizer for 300 epochs without learning rate scheduling. The weight decay was fixed at 10^{-4} and the batch size was set to 512. The experiments were run with Tesla V100-SXM2. For better generalization, we applied standard data augmentation technique, `RandomHorizontalFlip`, `RandomCrop`, and normalization to each image. The learning rate was selected from $\{10^{-3}, 5 \times 10^{-4}, 10^{-4}, 5 \times 10^{-5}, 10^{-5}\}$ using a 10% hold-out validation set. We selected the learning rate with the best classification accuracy on the validation dataset. Note that here we assumed the ordinary labels in the validation dataset are known. We will discuss other validation objectives that rely only on complementary labels in Section 6. As CLL algorithms are prone to overfitting [1, 10], some previous works did not use the model after training for evaluation. Instead, previous works were performed by evaluating the model on the validation dataset and selecting the epoch with the highest validation accuracy. In this work, we also follow the same aforementioned technique to validate testing set. For reference, we also performed the experiments on synthetically-generated CLL dataset, where the CLs were generated uniformly and noiselessly, denoted uniform-CIFAR.

Results and discussion As we can observe in Table 1, there is a significant performance gap between the humanly annotated dataset, CLCIFAR, and the synthetically generated dataset, uniform-CIFAR. The difference between the two datasets can be divided into three parts: (a) whether the generation of complementary labels depends on the feature, (b) whether there is noise, and (c) whether the complementary labels are generated with bias. A negative answer to those questions simplify the problem of CLL. We can gradually simplify CLCIFAR to uniform-CIFAR by chaining those assumptions as follows ⁴:

³Note that FWD-R and URE-GA-R assume the empirical transition matrix T_e to be provided. The empirical transition matrix is computed from the labels in the training set, so it is slightly different from a uniform transition matrix T_u in the uniform-CIFAR datasets. As a result, the performances of FWD-R and URE-GA-R do not exactly match those of FWD-U and URE-GA-U, respectively, in the uniform-CIFAR datasets.

⁴The “interpolation” between CLCIFAR and uniform-CIFAR does not necessarily have to be this way. For instance, one can remove the biasedness before removing the noise. We chose this order to reflect the advance of CLL algorithms. First, researchers address the uniform



In the following subsections, we will analyze how these three factors affect the performance of the CLL algorithms.

5.2 Feature dependency

In this experiment, we verified whether the performance gap resulted from the feature-dependent generation of practical CLs. Conceivably, even if two images belong to the same class, the distribution on the complementary labels could be different. On the other hand, the distributional difference could also be too small to affect model performance, e.g., if $P(\bar{y} | y, \mathbf{x}) \approx P(\bar{y} | y)$ for most \mathbf{x} . Consequently, we decided to further look into whether this assumption can explain the performance gap. To observe the effects of approximating $P(\bar{y} | y, \mathbf{x})$ with $P(\bar{y} | y)$, we generated two synthetic complementary datasets, CLCIFAR10-*iid* and CLCIFAR20-*iid* by i.i.d. sampling CLs from the empirical transition matrix in CLCIFAR10 and CLCIFAR20, respectively. We proceeded to benchmark the CLL algorithms on CLCIFAR-*iid* and presented the accuracy difference compared to CLCIFAR in Table 2.

Results and discussion From Table 2, we observed that the accuracy barely changes on the resampled CLCIFAR-*iid*, suggesting that even if the complementary labels in CLCIFAR could be feature-dependent, this dependency does not affect the model performance significantly. Hence, there might be other factors contributing to the performance gap.

Table 2: Mean accuracy difference (\pm standard deviation) of different CLL algorithms. A plus indicates the performance on is calculated as CLCIFAR-*i.i.d.* accuracy minus CLCIFAR accuracy.

	FWD-U	FWD-R	URE-GA-U	URE-GA-R	SCL-NL	SCL-EXP	L-W	L-UW	PC-sigmoid
<i>CLCIFAR10-iid</i>	-1.1 \pm 2.17	-0.36 \pm 1.15	-3.03 \pm 1.25	0.74 \pm 0.35	-0.67 \pm 1.81	-1.97 \pm 1.16	-2.5 \pm 0.56	-3.53 \pm 1.36	-2.03 \pm 2.05
<i>CLCIFAR20-iid</i>	-0.64 \pm 0.39	-3.53 \pm 1.13	-0.37 \pm 0.51	1.79 \pm 2.34	-0.28 \pm 0.61	-0.39 \pm 0.69	-0.5 \pm 1.37	-0.82 \pm 0.04	-2.24 \pm 0.52

5.3 Labeling noise

In this experiment, we further investigated the impact of the label noise on the performance gap. Specifically, we measured the accuracy on the noise-removed versions of CLCIFAR datasets, where varying percentages (0%, 25%, 50%, 75%, or 100%) of noisy labels are eliminated.

Results and discussion We present the performance of FWD trained on the noise-removed CLCIFAR10 dataset in the left figure in Figure 3. The results for other algorithms and the noise-removed CLCIFAR20 dataset can be found in

case [9], then generalize to the biased case [28], then consider noisy labels [11]. There is no work considering feature-dependent complementary labels yet.

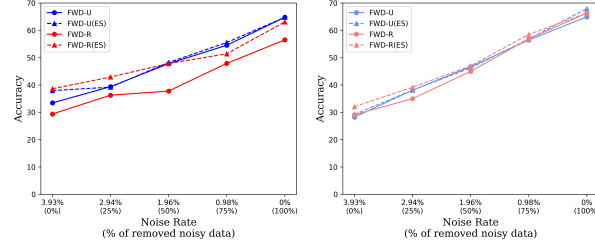


Figure 3: Accuracy of FWD-U and FWD-R on the noise-removed CLCIFAR10 dataset (**Left**) and the uniform-CIFAR10 dataset with uniform noise (**Right**) at varying noise rates.

Appendix E. From the figure, we observe a strong positive correlation between the performance and the proportion of removed noisy labels. When more noisy labels are removed, the performance gap diminishes and the accuracy approaches that of the ideal uniform-CLFAR dataset. Therefore, we conclude that the performance gap between the humanly annotated CLs and the synthetically generated CLs are primarily attributed to the label noise.

5.4 Biasedness of complementary labels

To further study the biasedness of CL as a potential factor contributing to the performance gap, we removed the biasedness from the noise-removed CLCIFAR dataset and examined the resulting accuracy. Specifically, we introduced the same level of uniform noise in uniform-CIFAR dataset and reevaluated the performance of FWD algorithms.

Results and discussion The striking similarity between the two curves in the right figure in Figure 3 shows that the accuracy is significantly influenced by label noise, while the biasedness of CL has a negligible impact on the results. Furthermore, we observe that the accuracy difference between the results of the last epoch and the best accuracy of validation set (or early-stopping: **ES**) results becomes smaller when the model is trained on the uniformly generated CLs. That is, the T -informed methods are more prone to overfitting when there is a bias in the CL generation.

With the experiment results in Section 5.2, 5.3, and 5.4, we can conclude that the performance gap between humanly annotated CL and synthetically generated CL is primarily attributed to label noise. Additionally, the biasedness of CLs may potentially contribute to overfitting, while the feature-dependent CLs do not detrimentally affect performance empirically. It is worth noting that in the last row of Table 1, the MAE methods that can learn from noisy CL fails to generalize well in the practical dataset. These results suggest that more research on learning with noisy complementary labels can potentially make CLL more realistic.

Table 3: The testing accuracy of models evaluated with URE and SCEL.

	CLCIFAR10				CLCIFAR20				CLMIN10				CLMIN20			
	URE	SCEL	valid acc	gap (↓)	URE	SCEL	valid acc	gap (↓)	URE	SCEL	valid acc	gap (↓)	URE	SCEL	valid acc	gap (↓)
FWD-U	33.13 \pm 1.30	31.86 \pm 1.52	34.83 \pm 0.50	1.70	6.70 \pm 0.46	7.10 \pm 0.48	8.03 \pm 0.74	0.93	20.75 \pm 2.12	20.20 \pm 0.72	23.85 \pm 2.76	3.10	4.97 \pm 0.72	4.55 \pm 0.81	6.33 \pm 1.04	1.35
FWD-R	33.70 \pm 1.38	35.64 \pm 1.37	38.13 \pm 0.88	2.49	17.35 \pm 2.32	18.40 \pm 1.56	20.27 \pm 0.53	1.86	22.15 \pm 4.15	29.15 \pm 1.93	30.15 \pm 1.83	1.00	8.60 \pm 1.32	9.90 \pm 1.19	10.60 \pm 0.82	0.70
URE-GA-U	30.45 \pm 1.58	33.21 \pm 1.12	34.72 \pm 0.40	1.51	7.03 \pm 0.61	8.71 \pm 0.74	10.49 \pm 0.52	1.79	17.05 \pm 3.35	21.30 \pm 3.01	22.90 \pm 2.97	1.60	4.27 \pm 0.80	5.03 \pm 0.48	5.75 \pm 0.43	0.72
URE-GA-R	27.39 \pm 1.09	28.32 \pm 1.38	30.23 \pm 0.70	1.91	3.58 \pm 0.47	5.42 \pm 0.96	6.17 \pm 0.82	0.75	8.90 \pm 1.03	10.30 \pm 1.53	13.25 \pm 1.11	2.95	5.15 \pm 0.62	5.57 \pm 1.54	6.50 \pm 0.35	0.93
SCL-NL	35.55 \pm 0.79	33.70 \pm 1.13	34.77 \pm 0.60	1.07	6.73 \pm 0.51	7.47 \pm 0.56	8.02 \pm 0.36	0.55	19.55 \pm 1.37	22.15 \pm 1.76	21.80 \pm 1.85	-0.35	4.85 \pm 1.12	5.20 \pm 0.51	6.17 \pm 0.40	0.98
SCL-EXP	31.30 \pm 2.62	33.47 \pm 1.16	35.18 \pm 0.67	1.71	6.83 \pm 0.23	7.03 \pm 0.62	7.70 \pm 0.41	0.66	18.35 \pm 1.60	20.65 \pm 1.39	24.80 \pm 1.14	4.15	5.05 \pm 0.56	4.45 \pm 0.74	5.58 \pm 0.13	0.52
L-W	27.49 \pm 4.30	30.32 \pm 2.40	32.99 \pm 1.01	2.67	5.90 \pm 0.29	7.18 \pm 0.31	7.71 \pm 0.35	0.53	19.30 \pm 4.66	18.95 \pm 2.30	23.80 \pm 2.64	4.50	5.97 \pm 0.33	5.55 \pm 0.17	6.40 \pm 0.29	0.43
L-UW	28.90 \pm 2.01	29.78 \pm 2.09	34.09 \pm 0.32	4.91	6.40 \pm 0.42	8.16 \pm 0.30	8.15 \pm 0.30	-0.01	18.25 \pm 4.31	19.80 \pm 1.61	22.40 \pm 1.67	2.60	5.82 \pm 0.77	6.48 \pm 1.03	6.35 \pm 0.86	-0.13
PC-sigmoid	24.83 \pm 5.94	31.48 \pm 1.93	32.15 \pm 0.80	0.67	7.98 \pm 2.47	10.50 \pm 0.37	12.11 \pm 0.46	1.51	12.55 \pm 1.31	17.85 \pm 4.61	23.15 \pm 0.46	5.30	6.40 \pm 1.19	5.53 \pm 1.28	6.90 \pm 1.04	0.50
ROB-MAE	18.80 \pm 1.64	18.75 \pm 0.90	20.23 \pm 1.02	1.43	4.70 \pm 0.43	4.87 \pm 0.32	5.40 \pm 0.59	0.53	11.80 \pm 2.92	14.35 \pm 1.59	14.15 \pm 0.68	-0.20	5.08 \pm 0.44	4.62 \pm 0.66	5.38 \pm 0.33	0.30

6 Validation Objectives

Validation is a crucial component in applying CLL algorithms in practice. With the collection of the real-world datasets, we are now able to estimate the difference between using ordinary labels for validation (the common practice in existing CLL studies, as what we do in Section 5) and using complementary labels for validation.

Validation objectives As discussed in Section 2, validating the model performance solely with complementary labels poses a non-trivial challenge. To the best of our knowledge, only two existing CLL studies offer some possibility to evaluate a classifier *with only complementary labels*. They are URE [10] and SCEL [15]. We take these two validation objectives to select the optimal learning rate from $\{10^{-3}, 5 \times 10^{-4}, 10^{-4}, 5 \times 10^{-5}, 10^{-5}\}$ and provides the accuracy on testing set in Table 3. We compare the result to another validation objective that computes the accuracy on an equal number of *ordinary labels*. Our goal was to determine the gap between using complementary labels and ordinary labels for validation. We selected the best learning rate based on the validation objectives for URE, SCEL, and ordinary-label accuracy, and then report the test performance, as shown in Table 3 for real-world datasets and Table 4 in the Appendix for synthetic datasets.

Results and discussion Firstly, there appears no clear winner between URE and SCEL, both using only CLs for validation. Validating with the ordinary-label accuracy generally provides stronger performance than URE/SCEL, and the test performance gap between validating with ordinary labels and validating with complementary labels can be as big as nearly 5%. These findings suggest that using purely complementary labels for validation, whether through URE or SCEL, still suffers from a non-negligible performance drop compared to using ordinary validation. That is, the numbers reported in existing studies, which validates with ordinal labels, can be optimistic for practice. Whether this gap can be further reduced remains an open research problem and the community can pay more attention on that to make CLL more practical.

7 Conclusion

In this paper, we devised a protocol to collect complementary labels from human annotators. Utilizing this protocol, we curated four real-world datasets,

CLCIFAR10, CLCIFAR20, CLMicroImageNet10, and CLMicroImageNet20 and made them publicly available to the research community. Through our meticulous analysis of these datasets, we confirmed the presence of noise and bias in the human-annotated complementary labels, challenging some of the underlying assumptions of existing CLL algorithms. Extensive benchmarking experiments revealed that noise is a critical factor that undermines the effectiveness of most existing CLL algorithms. Furthermore, the biased complementary labels can trigger overfitting, even for algorithms explicitly designed to leverage this bias information. In addition, our study on the validation objective for CLL suggests that validating with only complementary labels causes significant performance degrading. These findings emphasize the need for the community to dedicate more effort on those issues. The curated datasets pave the way for the community to create more practical and applicable CLL solutions.

References

- [1] Y.-T. Chou, G. Niu, H.-T. Lin, and M. Sugiyama. Unbiased risk estimators can mislead: A case study of learning with complementary labels, 2020.
- [2] T. Cour, B. Sapp, and B. Taskar. Learning from partial labels. *The Journal of Machine Learning Research*, 12:1501–1536, 2011.
- [3] E. D. Cubuk, B. Zoph, D. Mane, V. Vasudevan, and Q. V. Le. Autoaugment: Learning augmentation policies from data, 2019.
- [4] F. Denis. Pac learning from positive statistical queries. In *Algorithmic Learning Theory: 9th International Conference, ALT’98 Otzenhausen, Germany, October 8–10, 1998 Proceedings 9*, pages 112–126. Springer, 1998.
- [5] A. Dosovitskiy, L. Beyer, A. Kolesnikov, D. Weissenborn, X. Zhai, T. Unterthiner, M. Dehghani, M. Minderer, G. Heigold, S. Gelly, et al. An image is worth 16x16 words: Transformers for image recognition at scale. *arXiv preprint arXiv:2010.11929*, 2020.
- [6] B. Frénay and M. Verleysen. Classification in the presence of label noise: a survey. *IEEE transactions on neural networks and learning systems*, 25(5): 845–869, 2013.
- [7] Y. Gao and M.-L. Zhang. Discriminative complementary-label learning with weighted loss. In *International Conference on Machine Learning*, pages 3587–3597. PMLR, 2021.
- [8] K. He, X. Zhang, S. Ren, and J. Sun. Deep residual learning for image recognition. 2016.
- [9] T. Ishida, G. Niu, W. Hu, and M. Sugiyama. Learning from complementary labels. *Advances in neural information processing systems*, 30, 2017.

- [10] T. Ishida, G. Niu, A. K. Menon, and M. Sugiyama. Complementary-label learning for arbitrary losses and models, 2019.
- [11] H. Ishiguro, T. Ishida, and M. Sugiyama. Learning from noisy complementary labels with robust loss functions. *IEICE TRANSACTIONS on Information and Systems*, 105(2):364–376, 2022.
- [12] A. Kolesnikov, L. Beyer, X. Zhai, J. Puigcerver, J. Yung, S. Gelly, and N. Houlsby. Big transfer (bit): General visual representation learning. In *Computer Vision—ECCV 2020: 16th European Conference, Glasgow, UK, August 23–28, 2020, Proceedings, Part V 16*, pages 491–507. Springer, 2020.
- [13] A. Krizhevsky. Learning multiple layers of features from tiny images. *University of Toronto*, 05 2012.
- [14] Y. Le and X. S. Yang. Tiny imagenet visual recognition challenge. 2015.
- [15] W.-I. Lin and H.-T. Lin. Reduction from complementary-label learning to probability estimates. In *Proceedings of the Pacific-Asia Conference on Knowledge Discovery and Data Mining (PAKDD)*, May 2023.
- [16] W.-Y. Lin. Reduction from complementary-label learning to probability estimates. Master’s thesis, 2023.
- [17] S. Liu, Y. Cao, Q. Zhang, L. Feng, and B. An. Consistent complementary-label learning via order-preserving losses. In *International Conference on Artificial Intelligence and Statistics*, pages 8734–8748. PMLR, 2023.
- [18] M. Oquab, T. Darcet, T. Moutakanni, H. Vo, M. Szafraniec, V. Khalidov, P. Fernandez, D. Haziza, F. Massa, A. El-Nouby, et al. Dinov2: Learning robust visual features without supervision. *arXiv preprint arXiv:2304.07193*, 2023.
- [19] G. Patrini, A. Rozza, A. Menon, R. Nock, and L. Qu. Making deep neural networks robust to label noise: a loss correction approach. In *Proceedings of the IEEE conference on computer vision and pattern recognition*, 2017.
- [20] O. Russakovsky, J. Deng, H. Su, J. Krause, S. Satheesh, S. Ma, Z. Huang, A. Karpathy, A. Khosla, M. Bernstein, A. C. Berg, and L. Fei-Fei. Imagenet large scale visual recognition challenge. *Int. J. Comput. Vision*, 115(3), 2015.
- [21] M. Sugiyama, H. Bao, T. Ishida, N. Lu, T. Sakai, and G. Niu. *Machine learning from weak supervision: An empirical risk minimization approach*. MIT Press, 2022.
- [22] D.-B. Wang, L. Feng, and M.-L. Zhang. Learning from complementary labels via partial-output consistency regularization. In *IJCAI*, pages 3075–3081, 2021.

- [23] H.-H. Wang, W.-I. Lin, and H.-T. Lin. Clcifar: Cifar-derived benchmark datasets with human annotated complementary labels, 2023.
- [24] W. Wang, T. Ishida, Y.-J. Zhang, G. Niu, and M. Sugiyama. Learning with complementary labels revisited: The selected-completely-at-random setting is more practical.
- [25] W. Wang, T. Ishida, Y.-J. Zhang, G. Niu, and M. Sugiyama. Learning with complementary labels revisited: A consistent approach via negative-unlabeled learning. *arXiv preprint arXiv:2311.15502*, 2023.
- [26] J. Wei, Z. Zhu, H. Cheng, T. Liu, G. Niu, and Y. Liu. Learning with noisy labels revisited: A study using real-world human annotations, 2022.
- [27] Y. You, J. Huang, B. Wang, and Q. Tong. Rethinking one-vs-the-rest loss for instance-dependent complementary label learning.
- [28] X. Yu, T. Liu, M. Gong, and D. Tao. Learning with biased complementary labels, 2018.
- [29] Z.-H. Zhou. A brief introduction to weakly supervised learning. *National science review*, 5(1):44–53, 2018.

Appendix

A Limitations

To ensure the compatibility with previous CLL algorithms, our work focuses on image datasets based on CIFAR10/100, and TinyImageNet. It is worth investigating the real-world CLL datasets on larger datasets, such as ImageNet, and other domains. On the other hand, the proposed protocol focuses on collecting real-world complementary labels for analyzing the common assumptions on CLL. That said, it is also crucial to understand efficient ways to collect complementary labels in practice, e.g., by asking annotators binary questions to collect ordinary and complementary labels simultaneously. We leave these directions as future works and hope that our work can open the way for the community to understand these questions.

B More discussion on practical noise and extended ablation study

Our work found out that the labeling noise is the main factor contributing to the performance gap between synthetic CL and practical CL. Hence, we conducted deeper investigation into some directions to handle the practical noise. In Section B.1, we discussed the performance improvement when more human-annotated complementary labels were available. In Section B.2, we designed the synthetic CLCIFAR-N dataset to study the difference between synthetic uniform noise and practical noise. In Section B.3, we provided the benchmark results of all robust loss methods to emphasize the essence of studying a practical complementary label dataset. In Section B.4, we discussed result analysis of CLCIFAR20 and CLMicroImageNet20 datasets and described the process how MicroImageNet10 and MicroImageNet20 datasets generation in Section B.5.

B.1 Multiple complementary labels

In this experiment, we studied the case when there were multiple CLs for a data instance. We duplicated the data instance and assigned them with another practical label from the annotators. The results of this experiment were summarized in Table 5.

For CLCIFAR10, we observe that the model achieved better learning performance when trained on data instances with more CLs. However, the issue of overfitting persists even with the increased number of labels. In the case of CLCIFAR20, we found that without employing early stopping techniques, it is challenging to achieve improved results as the number of labels increased. Furthermore, the overfitting problem becomes more pronounced with the increased number of labels. Overall, these findings shed light on the challenges posed by multiple CLs and the persistence of overfitting.

B.2 Benchmarks with synthetic noise

Generation process of CLCIFAR-N Inspired by the conclusions drawn in Section 5.3, we investigated another avenue of research: the generalization capabilities of methods when transitioning from synthetic datasets with uniform noise to practical datasets. To obtain a general synthetic dataset with minimum assumption, we introduced CLCIFAR-N. This synthetic dataset contains unifrom CL and uniform real world noise from CLCIFAR dataset. The complementary labels of CLCIFAR-N are *i.i.d.* sampled from T_{syn} , where the diagonal entries are set to be 3.93%/10 (for generating CL for CIFAR10) or 2.8%/20 (for generating CL for CIFAR20). The non-diagonal entries are uniformly distributed. This construction allows us to generate a synthetic dataset that mimics real-world scenarios more closely with minimum knowledge.

Benchmark results We ran the benchmark experiments with the identical settings as in Section 5.1 and present the results in Table 6. The performance difference between sythetic noise and practical noise are illustrated in the *diff* columns. A smaller difference indicates a better generalization capability of the models. Interestingly, the robust loss methods exhibit superiority on the synthetic CLCIFAR10-N dataset but struggle to generalize well on real-world datasets. This finding suggests the existence of fundamental differences between synthetic noise and practical noise. Further investigation into these differences is left as an avenue for future research.

Table 4: The testing accuracy of models evaluated with URE and SCEL.

	uniform-CIFAR10				uniform-CIFAR20				uniform-MIN10				uniform-MIN20			
	URE	SCEL	valid acc	gap (↓)	URE	SCEL	valid acc	gap (↓)	URE	SCEL	valid acc	gap (↓)	URE	SCEL	valid acc	gap (↓)
FWD-U	53.41 \pm 5.51	50.36 \pm 3.35	64.19 \pm 0.57	10.78	16.73 \pm 2.29	16.52 \pm 2.61	21.54 \pm 0.37	4.81	33.65 \pm 2.84	33.20 \pm 3.16	36.30 \pm 1.12	2.65	10.10 \pm 2.66	9.15 \pm 1.68	12.57 \pm 2.94	2.47
FWD-R	52.55 \pm 4.06	49.17 \pm 3.11	61.32 \pm 0.90	8.77	18.29 \pm 0.39	16.61 \pm 2.65	21.50 \pm 0.38	3.21	32.15 \pm 3.40	33.10 \pm 2.03	35.70 \pm 1.19	2.60	12.72 \pm 3.28	11.57 \pm 2.91	14.85 \pm 1.75	2.12
URE-GA-U	48.68 \pm 1.11	49.29 \pm 1.67	50.24 \pm 1.11	0.95	15.23 \pm 2.35	16.09 \pm 1.23	16.67 \pm 1.35	0.58	28.10 \pm 5.24	34.35 \pm 2.39	35.70 \pm 1.97	1.35	8.53 \pm 1.55	8.52 \pm 1.38	11.65 \pm 1.90	3.12
URE-GA-R	50.40 \pm 1.21	50.25 \pm 1.57	50.73 \pm 1.83	0.25	15.68 \pm 1.35	16.12 \pm 0.95	17.57 \pm 0.61	1.45	29.85 \pm 4.73	34.10 \pm 1.90	33.65 \pm 1.40	-0.45	7.15 \pm 2.13	7.12 \pm 2.42	9.78 \pm 3.88	2.63
SCL-NL	54.32 \pm 6.71	51.03 \pm 3.12	63.76 \pm 0.09	9.44	15.65 \pm 3.06	16.32 \pm 3.11	21.37 \pm 1.18	5.05	32.95 \pm 3.13	33.20 \pm 3.69	37.05 \pm 1.40	3.85	11.50 \pm 3.76	9.28 \pm 2.55	13.00 \pm 2.80	1.50
SCL-EXP	50.98 \pm 6.83	41.61 \pm 3.52	63.29 \pm 1.02	12.30	16.71 \pm 2.72	16.15 \pm 2.55	21.57 \pm 1.13	4.86	32.95 \pm 2.91	29.70 \pm 2.83	36.55 \pm 1.28	3.60	10.53 \pm 2.02	8.83 \pm 3.19	12.95 \pm 3.38	2.43
L-W	46.88 \pm 9.44	50.36 \pm 0.47	54.32 \pm 0.41	3.95	16.26 \pm 1.93	14.67 \pm 1.59	19.59 \pm 0.99	3.33	17.70 \pm 3.90	28.60 \pm 5.15	33.80 \pm 2.66	5.20	8.58 \pm 1.25	7.70 \pm 0.35	12.70 \pm 2.35	4.12
L-UW	52.47 \pm 3.83	51.15 \pm 1.81	57.52 \pm 0.59	5.05	16.10 \pm 1.31	15.58 \pm 1.97	20.71 \pm 0.92	4.62	22.10 \pm 7.66	25.60 \pm 7.14	35.10 \pm 2.74	9.50	10.60 \pm 2.96	8.28 \pm 2.02	12.12 \pm 3.13	1.52
PC-sigmoid	35.29 \pm 1.67	34.82 \pm 1.24	37.78 \pm 0.80	2.49	13.41 \pm 0.95	13.40 \pm 0.72	14.48 \pm 0.47	1.07	25.55 \pm 5.99	27.05 \pm 5.66	29.10 \pm 0.98	2.05	7.75 \pm 1.73	8.72 \pm 0.26	10.72 \pm 1.38	2.00
ROB-MAE	57.99 \pm 1.72	57.79 \pm 2.03	59.38 \pm 0.63	1.39	17.07 \pm 2.02	15.62 \pm 1.79	18.17 \pm 1.31	1.11	30.15 \pm 4.22	29.15 \pm 2.90	31.50 \pm 1.81	1.35	5.42 \pm 0.27	5.03 \pm 0.54	6.35 \pm 0.86	0.92

B.3 Results of the robust loss methods

The original design of the robust loss aims to obtain the optimal risk minimizer even in the presence of corrupted labels. However, their methods do not generalized well on practical datasets. The results are provided in Table 7. In other words, solely considering synthetic noisy CLs does not guarantee performance on real-world datasets. These results once again underscore the importance of the CLCIFAR dataset.

B.4 Result analysis of CLCIFAR20 and MicroImageNet20

In this section, we further investigate the complementary labels collected from the CLCIFAR20 and MicroImageNet20 datasets. We followed similar observation

Table 5: Learning with Multiple CL: The figure shows the classification accuracy of each task with early stopping indicated in brackets. The highest accuracy in each column is bolded for ease of comparison.

num CL	CLCIFAR10			CLCIFAR20		
	1	2	3	1	2	3
FWD-U	34.09(36.83)	41.95(41.53)	42.88(45.18)	7.47(8.27)	8.28(8.78)	8.15(10.27)
FWD-R	28.88(38.9)	34.33(47.07)	37.84(49.76)	16.14(20.31)	16.99(23.41)	15.54(24.19)
URE-GA-U	34.59 (36.39)	45.71 (44.85)	45.97 (47.97)	7.59(10.06)	8.42(11.52)	8.53(12.75)
URE-GA-R	28.7(30.94)	42.73(43.34)	44.73(47.36)	5.24(5.46)	6.77(6.92)	5.0(5.55)
SCL-NL	33.8(37.81)	40.67(42.58)	43.39(45.2)	7.58(8.53)	6.77(6.92)	5.0(5.55)
SCL-EXP	34.59 (36.96)	40.89(42.99)	44.4(47.9)	7.55(8.11)	7.42(8.39)	8.0(9.31)
L-W	28.04(34.55)	34.96(41.83)	39.05(47.46)	7.08(8.74)	8.06(8.76)	8.03(10.18)
L-UW	30.63(35.13)	38.05(43.32)	39.49(45.82)	7.36(8.71)	7.03(8.55)	7.86(10.11)
PC-sigmoid	24.38(35.88)	25.63(39.82)	33.89(43.75)	9.27(14.26)	11.91(16.07)	17.68 (14.13)

Table 6: Benchmark results on CLCIFAR-N datasets. The classification accuracy difference is calculated by subtracting the practical CLCIFAR dataset from the performance on the synthetic CLCIFAR-N dataset.

	CLCIFAR10-N	diff(\downarrow)	CLCIFAR20-N	diff(\downarrow)
FWD-U	37.1	2.2	7.58	0.11
FWD-R	-	-	-	-
URE-GA-U	31.29	-3.3	8.1	0.5
URE-GA-R	-	-	-	-
SCL-NL	37.79	2.06	7.75	0.16
SCL-EXP	35.86	3.19	6.95	-0.59
L-W	30.1	2.06	6.16	-0.91
L-UW	32.69	2.05	6.89	-0.47
PC-sigmoid	19.64	-4.73	6.54	-2.72
CCE	32.34	13.45	5.71	0.71
MAE	41.34	23.09	6.83	1.83
WMAE	37.62	22.26	6.36	1.08
GCE	35.00	18.71	6.7	1.7
SL	29.98	12.29	6.08	1.05

and analyzed in the Section 4. Our observation and analysis are described as below:

Observation 1: noise rate compared to ordinary label collection We observed that the noise rates for the complementary labels collected from the CLCIFAR20 and MicroImageNet20 datasets are 2.80% and 3.21%, respectively. This finding is consistent with the observations discussed in Section 4. The lower noise rate in the CLCIFAR20 dataset compared to MicroImageNet20 can be attributed to the greater difficulty in labeling the MicroImageNet20 dataset.

Observation 2: imbalanced complementary label annotation Next, we analyzed the distribution of the collected complementary labels. The frequencies of these labels for the CLCIFAR20 and CLMicroImageNet20 (CLMIN20) datasets are shown in Figure 4. The figure reveals that annotators exhibit specific biases towards certain labels. For example, in CLCIFAR20, annotators show a preference for labels such as "fish", "flowers", "people", "trees", "food container", and "transportation vehicles". In CLMIN20, they favor "iPod" and "tractor". In CLCIFAR20, the bias tends towards labels with shorter, more concrete, and understandable names. Conversely, in CLMIN20, the preference is for easily recognizable items as "iPod", and "tractor", while less familiar items such as

Table 7: Standard benchmark results on CLCIFAR and uniform-CIFAR datasets for the robust loss method. Mean accuracy (\pm standard deviation) on the testing dataset from four trials with different random seeds. Highest accuracy in each column is highlighted in bold.

	uniform-CIFAR10		CLCIFAR10		uniform-CIFAR20		CLCIFAR20	
methods	valid_acc	valid_acc (ES)	valid_acc	valid_acc (ES)	valid_acc	valid_acc (ES)	valid_acc	valid_acc (ES)
CCE	46.57 \pm 1.75	49.51 \pm 0.73	16.18 \pm 2.97	20.18 \pm 3.39	12.54 \pm 0.40	14.62 \pm 1.29	5.07 \pm 0.05	5.41 \pm 0.30
MAE	57.37 \pm 0.48	58.50 \pm 0.97	16.30 \pm 2.27	19.44 \pm 4.41	16.72 \pm 1.52	17.63 \pm 1.63	5.11 \pm 0.11	5.87 \pm 0.26
WMAE	-	-	13.01 \pm 1.89	15.51 \pm 0.75	-	-	5.31 \pm 0.27	6.65 \pm 0.65
GCE	58.10 \pm 1.54	59.44 \pm 2.30	14.31 \pm 1.44	18.97 \pm 2.16	15.86 \pm 1.93	17.09 \pm 1.19	5.21 \pm 0.29	5.76 \pm 0.32
SL	41.13 \pm 1.64	42.64 \pm 0.11	16.45 \pm 2.80	19.28 \pm 3.16	13.60 \pm 0.55	15.70 \pm 1.23	5.44 \pm 0.29	6.59 \pm 0.43

"bannister", "american lobster", "snorkel", and "gazelle" are less favored.

Observation 3: biased transition matrix Finally, we visualized the empirical transition matrix using the collected complementary labels, as shown in Figure 5. Our observations indicate that the transition matrix is biased. Specifically, we discovered that the bias in the complementary labels is dependent on the true labels, as depicted in Figure 5. In CLCIFAR20, there are more annotations for labels with shorter, more concrete, and understandable names, such as "fish," "flowers," "people," and "transportation vehicles." This results in a distribution that is more biased towards these labels. A similar pattern of bias is observed in CLMIN20, where annotators favored easily recognizable items like "iPod" and "tractor", while less familiar items received fewer annotations.

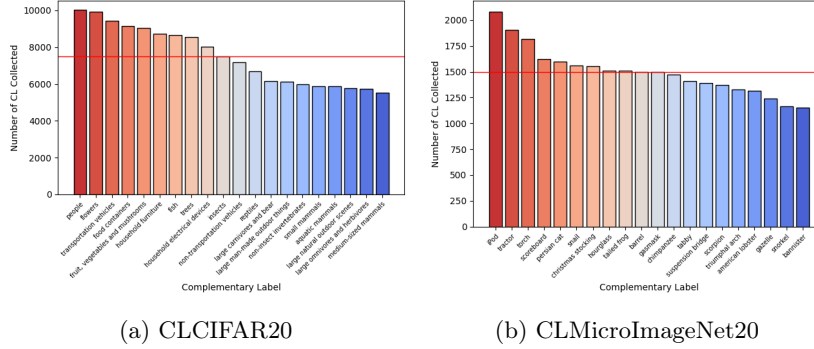


Figure 4: The label distribution of CLCIFAR20 and CLMicroImageNet20 datasets.

B.5 MicroImageNet dataset generation

To generate the MicroImageNet10 and MicroImageNet20 datasets, we began by randomly selecting 10 classes from the 200 available in MicroImageNet to create MicroImageNet10. Similarly, we randomly selected 20 classes to form MicroImageNet20. The selected classes are listed in Table 10 of Appendix F. Each class in the TinyImageNet200 dataset contains multiple labels. To ensure

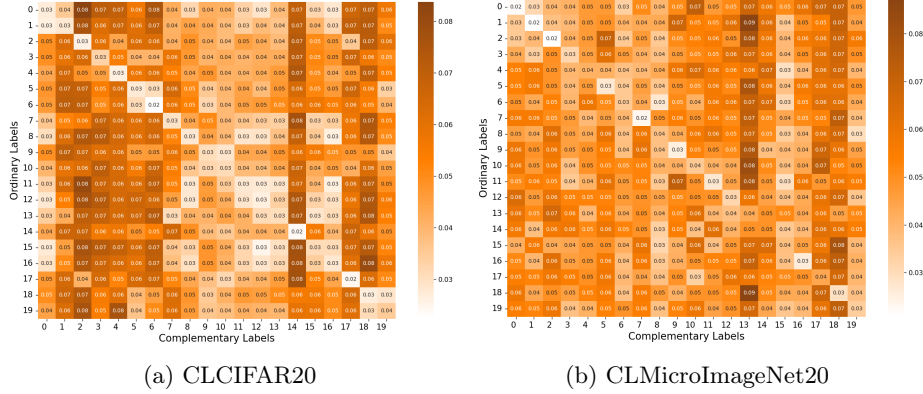


Figure 5: The empirical transition matrices of CLCIFAR20 and CLMicroImageNet20. The label names of CLCIFAR20 and CLMicroImageNet20 are abbreviated as indexes to save space. The full label names are provided in Appendix F.

reproducibility and facilitate human annotation, we chose the first label to represent the primary label of each class, as detailed in Appendix F. Each class in the MicroImageNet10/20 datasets comprises 500 images for the training set and 50 images for the validation set. To collect complementary labels for the MicroImageNet10/20 datasets, we followed a protocol similar to the one described in Section 3.2.

C More discussion on biasedness

In addition to the label noise, the biasedness of CL in practical dataset would lead to overfitting, especially for those T-informed algorithms. We conducted deeper investigation into this phenomenon. In Section C.1, we demonstrated the necessity of employing data augmentation techniques to prevent overfitting. In Section C.2, we attempted to address the issue of overfitting by employing an interpolated transition matrix for regularization.

C.1 Ablation on data augmentation

To further investigate the significance of data augmentation, we conducted identical experiments without employing data augmentation during the training phase. As we can observe in the training curves in Figure 6, data augmentation could improve the testing accuracy of all the algorithms we considered.

We also provide the results without the use of data augmentation techniques in Table 8, and we observed that almost all methods suffered from overfitting. It is worth noting that URE with gradient ascent suffers less compared to the other methods. The reason might be that reversing the gradient of the class with negative loss (the overfitting class) can be seen as a regularization technique.

Table 8: The overfitting results when there is no data augmentation.

	uniform-CIFAR10		CLCIFAR10		uniform-CIFAR20		CLCIFAR20	
methods	valid_acc	valid_acc (ES)	valid_acc	valid_acc (ES)	valid_acc	valid_acc (ES)	valid_acc	valid_acc (ES)
FWD-U	48.44	49.33	21.29	25.59	17.4	17.97	6.91	7.32
FWD-R	-	-	14.97	28.3	-	-	6.82	14.67
URE-GA-U	39.55	39.67	21.0	23.53	13.52	14.08	5.55	8.38
URE-GA-R	-	-	19.81	20.8	-	-	5.0	6.43
SCL-NL	48.2	48.27	21.96	26.51	16.55	17.54	7.1	7.92
SCL-EXP	46.79	47.52	21.89	27.66	16.18	17.89	6.9	7.3
L-W	27.02	44.78	20.06	27.6	10.39	16.3	5.64	8.02
L-UW	31.3	46.38	20.28	26.26	12.33	16.32	6.03	8.14
PC-sigmoid	18.97	33.26	-	-	7.67	10.41	-	-

Therefore, URE with GA methods can be more resistant to overfitting in practical datasets.

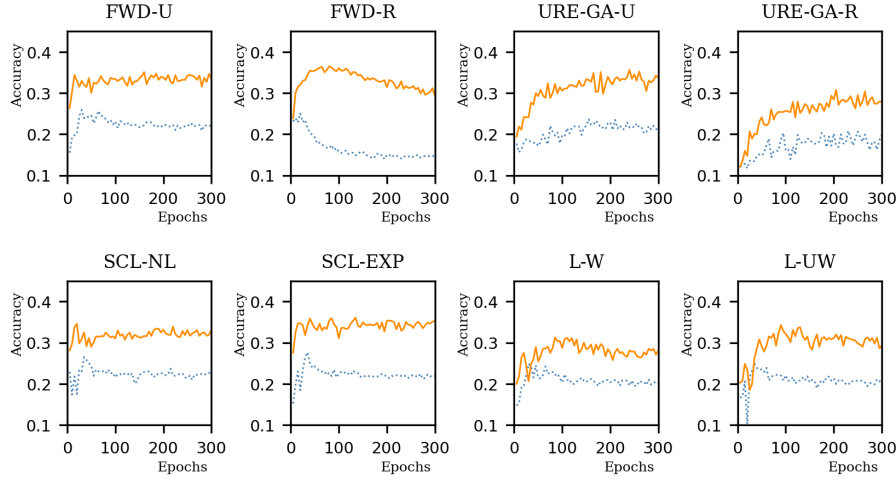


Figure 6: The Overfitting accuracy curve of FWD, URE, SCL-NL, L-W. The dotted line represents the accuracy obtained without data augmentation, while the solid line represents the accuracy with data augmentation included for reference. The accuracy of FWD, SCL-NL, SCL-EXP, L-W, L-UW methods reaches its highest at approximately the 50 epoches and converges to some lower point. The detail numbers are in Table 8

C.2 Ablation on interpolation between T_u and T_e

In Table 1, we discovered that the T -informed methods did not always deliver better testing accuracy when T_e is given. Looking at the difference between the accuracy of using early-stopping and not using early-stopping, we observe that when the T_u is given to the T -informed methods, the difference becomes smaller. This suggests that T -informed methods using the empirical transition matrix has greater tendency to overfitting. On the other hand, T -informed methods

using the uniform transition matrix could be a more robust choice.

We observe that the uniform transition matrix T_u acts like a regularization choice when the algorithms overfit on CLCIFAR. This results motivate us to study whether we can interpolate between T_u and T_e to let the algorithms utilize the information of transition matrix while preventing overfitting. To do so, we provide an interpolated transition matrix $T_{\text{int}} = \alpha T_u + (1 - \alpha)T_e$ to the algorithm, where α controls the scale of the interpolation. As FWD is the T -informed method with the most severe overfitting when using T_u , we performed this experiment using FWD and reported the results in Figure 7. As shown in Figure 7, FWD can learn better from an interpolated T_{int} , confirming the conjecture that T_u can serve as a regularization role.

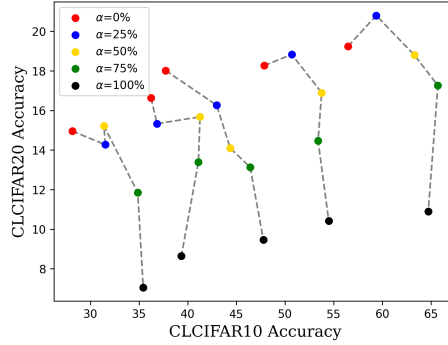


Figure 7: The last epoch accuracy of CLCIFAR10 and CLCIFAR20 for FWD algorithm with an α -interpolated transition matrix T_{int} . The five solid points on each curve represent different noise cleaning rate: 0%, 25%, 50%, 75%, 100% from left to right.

D An overview of the complementary-label learning algorithms

In this section, we review the algorithms benchmarked in Section 5.

D.1 T-informed CLL algorithms

Some of them take the transition matrix T as inputs, which we call T -informed methods, including

- Two versions of forward correction method [28]: **FWD-U** and **FWD-R**. They utilize a uniform transition matrix T_u and an empirical transition matrix T_e as input, respectively.
- Two versions of unbiased risk estimator with gradient ascent [10]: **URE-GA-U** with a uniform transition matrix T_u and **URE-GA-R** with an

empirical transition matrix T_e .

- Robust loss methods [11] for learning from noisy CL, including **CCE**, **MAE**, **WMAE**, **GCE**, and **SL**⁵. We applied the gradient ascent technique [10] as recommended in the original paper.

In practice, the empirical transition matrix T_e is not accessible to the learning algorithm, but we assume that the correct T_e is given to **FWD-R**, **URE-GA-R** and the robust loss methods for simplicity.

T-informed CLL algorithms are those that has the transition matrix as inputs, includes but not limited to Forward loss correction (FWD) and Unbiased risk estimate (URE). They are expected to utilize the information of the transition matrix to provide better performance when the complementary labels are not generated uniformly. The transition matrix, however, may not be accessible in practice. In this case, a uniform transition matrix T_u is typically provided to the algorithms as a default choice. In the benchmark in Section 5, we considered both scenarios in which the empirical transition matrix T_e or the uniform transition matrix T_u was provided.

FWD Forward loss correction utilizes the information of a transition matrix T in its loss function as in Eq. 3 [28]. Essentially, this method trains model f by minimizing the following loss function.

$$R(\mathbf{g}) = \frac{1}{N} \sum_{i=1}^N \ell(T^\top \text{sm}(\mathbf{g}(x_i)), \bar{y}_i) \quad (3)$$

where T is the transition matrix provided to the method and sm denotes the softmax function. We use **FWD-U** and **FWD-R** to indicate the cases that T equals T_u and T_e , respectively.

URE-GA Ishida et al. [9] proposed an unbiased risk estimator (URE) for learning from complementary label. The loss of the URE is defined as follows,

$$R(\mathbf{g}) = \frac{1}{N} \sum_{i=1}^N e_{\bar{y}_i}^\top (T^{-1}) \ell(\mathbf{g}(x_i)) \quad (4)$$

URE, however, can go below zero during the optimization procedure, leading to overfitting of the model. To address this issue, Ishida et al. [10] proposed two tricks, non-negative risk estimator (NN) and gradient accent (GA). The former zeros out the gradient when the mini-batch loss goes below zero while the latter reverse the mini-batch gradient when the loss from any of the complementary class goes below zero. We replace the transition matrix T in the risk estimator 4 with T_u and T_e for **URE-GA-U** and **URE-GA-R**.

⁵Due to space limitations, we only provided the results of MAE. The remaining results and discussions related to the robust loss methods can be found in Appendix B.3.

D.2 T-agnostic CLL algorithms

T-agnostic CLL algorithms are those that do not take the information of the transition matrix, includes but not limited to Surrogate complementary loss (SCL) and Discriminative modeling (L-W/L-UW).

SCL Chou et al. [1] proposed to use the surrogate complementary loss (SCL) to address the overfitting tendency in URE. The loss function is defined as follows,

$$R(\mathbf{g}) = \frac{1}{N} \sum_{i=1}^N \phi(\bar{y}_i, \mathbf{g}(x_i)), \quad (5)$$

where $\phi(\cdot)$ is a surrogate loss for 0 – 1 loss. For instance, SCL-NL uses the negative log loss $\phi(\bar{y}, \mathbf{g}(\mathbf{x})) = -\log(1 - p_{\bar{y}})$ and SCL-EXP uses the exponential loss $\phi(\bar{y}, \mathbf{g}(\mathbf{x})) = \exp(p_{\bar{y}})$.

L-W/L-UW Gao and Zhang [7] proposed to use discriminative modeling to directly model the distribution of complementary labels. To do so, they proposed the following loss functions,

$$R(\mathbf{g}) = \frac{1}{N} \sum_{i=1}^N -\log(\text{sm}(1 - \text{sm}(\mathbf{g}(x))))_{\bar{y}_i}, \quad (6)$$

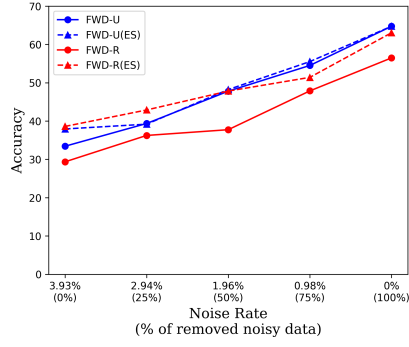
where sm denotes the softmax function. They also proposed a weighting function to further improve the performance. The unweighted version is denoted as L-UW and the weighted version is denoted as L-W.

D.3 Robust loss methods

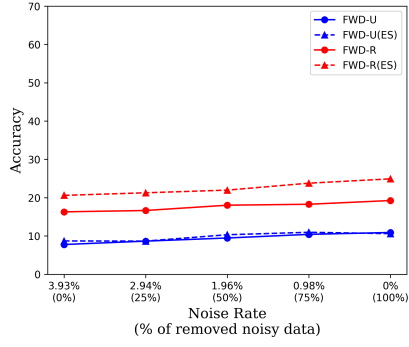
Ishiguro et al. [11] studied two conditions on loss functions: weighted symmetric condition and relaxation of weighted symmetric condition. Five loss functions that can be robust against the estimation error of the transition matrix were proposed. Their results can be further generalized to noisy complementary label learning. More experiment details for reproduction can be found in their paper.

E Additional charts for CLCIFAR dataset with data cleaning

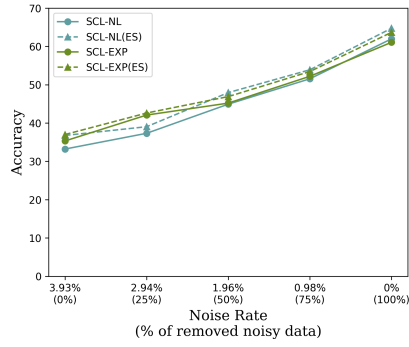
We remove 0%, 25%, 50%, 75%, 100% of the noisy data in CLCIFAR10 and CLCIFAR20 datasets. We discover that by removing the noisy data in the practical dataset, the practical performance gaps vanish for all the CLL algorithms. Therefore, we can conclude that the main obstacle to the practicality of CLL is label noise.



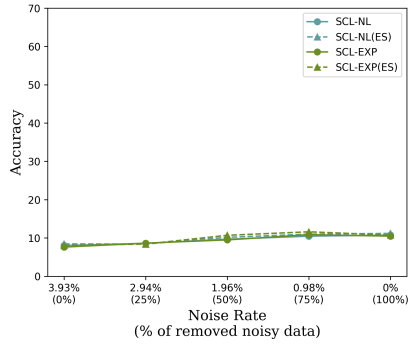
(a) FWD-(U/R) on CLCIFAR10



(b) FWD-(U/R) on CLCIFAR20



(a) SCL-(NL/EXP) on CLCIFAR10



(b) SCL-(NL/EXP) on CLCIFAR20

F Label names of CLCIFAR20 and CLMicroImageNet20

Table 9: The correspondence between index and label names of CLCIFAR20 and CLMicroImageNet20 datasets.

Index	CLCIFAR20 Label Name	CLMicroImageNet20 Label Name
0	aquatic mammals	tailed frog
1	fish	scorpion
2	flowers	snail
3	food containers	american lobster
4	fruit, vegetables and mushrooms	tabby
5	household electrical devices	persian cat
6	household furniture	gazelle
7	insects	chimpanzee
8	large carnivores and bear	bannister
9	large man-made outdoor things	barrel
10	large natural outdoor scenes	christmas stocking
11	large omnivores and herbivores	gasmask
12	medium-sized mammals	hourglass
13	non-insect invertebrates	iPod
14	people	scoreboard
15	reptiles	snorkel
16	small mammals	suspension bridge
17	trees	torch
18	transportation vehicles	tractor
19	non-transportation vehicles	triumphal arch

Table 10: The selected classes/folders for MicroImageNet10 (MIN10) and MicroImageNet20 (MIN20) are drawn from the TinyImageNet200 dataset. The labels provided in the table represent the **first** ordinary label for these classes.

Index	MIN10 Folder	MIN10 Label Name	Index	MIN20 Folder	MIN20 Label Name
0	n02281406	sulphur-butterfly	0	n01644900	tailed frog
1	n02769748	backpack	1	n01770393	scorpion
2	n02963159	cardigan	2	n01944390	snail
3	n03617480	kimono	3	n01983481	american lobster
4	n03706229	magnetic-compass	4	n02123045	tabby
5	n03838899	oboe	5	n02123394	persian cat
6	n04133789	scandal	6	n02423022	gazelle
7	n04456115	torch	7	n02481823	chimpanzee
8	n07873807	pizza	8	n02788148	bannister
9	n09193705	alp	9	n02795169	barrel
			10	n03026506	christmas stocking
			11	n03424325	gasmask
			12	n03544143	hourglass
			13	n03584254	iPod
			14	n04149813	scoreboard
			15	n04251144	snorkel
			16	n04366367	suspension bridge
			17	n04456115	torch
			18	n04465501	tractor
			19	n04486054	triumphal arch

G Analysis between multiple label collection trials

We carried out the same protocol for three independent trials to ensure the consistency of our results. The noise rates of CLCIFAR10 are 0.0398, 0.03882, and 0.03928 for three trials respectively. On the other hand, the noise rates of CLCIFAR20 are 0.02322, 0.02902, and 0.03196. These results show that the obtained noise rates are reliable and consistent. Besides, we also analyzed the distribution of complementary label within three trials as reported in Figure 10. The consistent distribution of complementary labels reveals the empirical human annotating biasedness within our protocol. Both analyses show that our protocol and discovery are solid and stable.

H AutoAugment

In addition to the standard data augmentation, RandomCrop and RandomHorizontalFlip, we also considered a more advanced one, AutoAugment [3]. The benchmark results using AutoAugment are provided in Table 11. We observe

